Carbon Nanotubes and Optical Confinement – Controlling Light Emission in Nanophotonic Devices

Mathias Steiner*[a], Fengnian Xia[a], Huihong Qian[b], Yu-Ming Lin[a], Achim Hartschuh[b], Alfred J. Meixner[c], Phaedon Avouris[a]
[a]IBM T. J. Watson Research Center, 1101 Kitchawan Road, Yorktown Heights, NY, USA 10598
[b]Department Chemie und Biochemie and CeNS, Ludwig-Maximilians-Universität München, Butenandtstrasse 5-13 E, München, Germany D-81377
[c]Institut für Physikalische und Theoretische Chemie, Eberhard-Karls-Universität Tübingen, Auf der Morgenstelle 8, Tübingen, Germany D-72076

ABSTRACT

We report here recent progress in nanophotonics with single-wall carbon nanotubes (SWNTs). A photonic model structure, the planar λ/2-microcavity, modifies the photonic density of modes at the location of the embedded SWNTs. As a result, the radiative properties of the SWNTs are modified due to the enhancement or inhibition of the microcavity-controlled spontaneous emission (scattering) rate. We use single-molecule optical microscopy and spectroscopy to investigate individual SWNTs (bundles), spatially isolated and immobilized in the photonic structure, and to measure the microcavity-controlled emission (Raman and photoluminescence) characteristics. Ultimately, we demonstrate experimentally that the integration of a field-effect transistor (FET) based on a single, semiconducting SWNT with a λ/2-microcavity results in a strong spectral and angular narrowing of the electrically excited and cavity-enhanced infrared radiation emitted by the nano-light source. Integrated nanophotonic devices based on carbon nanotubes hold great promise for application in quantum optics and optical communication.

Keywords: Carbon Nanostructures, Nano-Optics, Raman Scattering, Photoluminescence, Electroluminescence, Optoelectronics, Spontaneous Emission Enhancement, Purcell-Effect

1. INTRODUCTION

The family of single wall carbon nanotubes (SWNTs) constitutes a system of one-dimensional model structures exhibiting unique electronic and optical properties [1]. Semiconducting SWNTs can be utilized as active channels in truly nanosized field effect transistors (FETs) [2] and their excited states form strongly bound excitons. These excitons can be populated by either optical or electrical pumping and give rise to luminescence emission in the near infrared spectral regime [3]. Due to an extraordinarily large Raman scattering cross section, SWNTs can be investigated and characterized on the single-tube level using optical microscopy and spectroscopy [4], even after device integration [5].

Embedding SWNTs in optical microcavities is a promising way to further improve their radiative properties [6-8]. The efficiency of spontaneous radiative transitions in optical λ/2-microcavities, i. e. cavities with mirror spacings L of one half emission wavelength λ of the embedded emitters, is determined by the local photonic mode density $\rho_{cav}(L)$, that can be enhanced or inhibited with respect to the corresponding value ρ_0 in free (non-confined) space. (See e. g. [9] and references therein.) Accordingly, both photoluminescence and Raman scattering processes of embedded emitters can be controlled by enhancement [10] or inhibition [11] of the spontaneous emission rate Γ_{cav} or the Raman scattering cross section σ_{cav} [12,13], respectively, since $\Gamma_{cav}(L)/\Gamma_0 = \sigma_{cav}(L)/\sigma_0 \propto \rho_{cav}(L)/\rho_o$ [14].

*msteine@us.ibm.com; phone 1-914-945-2400

In the following, we show how to modify the radiative properties of SWNTs by integrating them with a planar λ/2-microcavity made of two metal mirrors. We use the modified photonic mode density within the cavity to selectively enhance or inhibit different Raman transitions of SWNTs and the measured spectra exhibit single Raman bands only. We demonstrate experimentally the microcavity-controlled photoluminescence of spatially isolated and immobilized SWNTs (bundles) and find a linear excitation power dependence for both Raman (G-band) and photoluminescence intensities. Finally, we discuss the on-chip integration of a FET based on an individual, semiconducting SWNTs and a λ/2-microcavity, an important step in nanophotonics and optoelectronics with SWNTs.

2. RESULTS AND DISCUSSION

2.1 Optically excited, microcavity-controlled emission of SWNTs

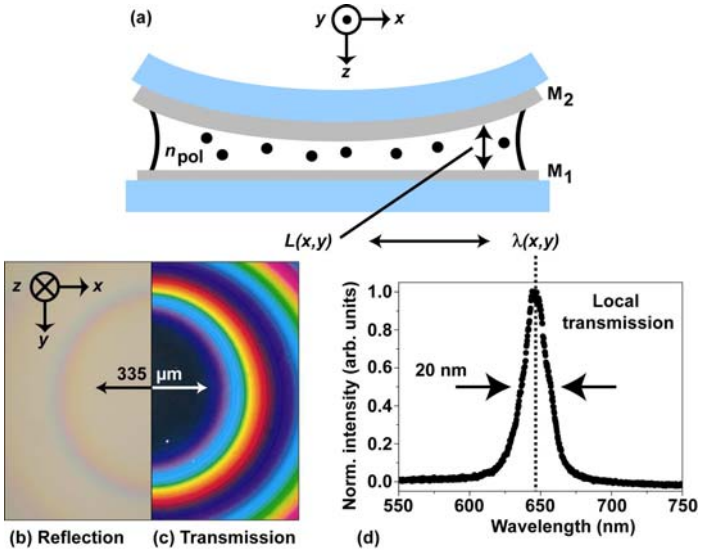

Fig. 1. Optical microcavity doped with single-wall carbon nanotubes (SWNTs). (a) The sample consists of two mirrors $M_{1,2}$ prepared by evaporating silver films onto glass coverslips (actual mirror parameters: thickness d_1 =30 nm, d_2= 60 nm; reflectivities R_1 = 0.7, R_2 = 0.9 at λ=532 nm for perpendicular incidence). The mirrors are separated by a layer of a transparent polymer (PMMA) with varying thickness enclosing homogenously distributed and randomly oriented SWNTs that are indicated by dots. Optical micrographs show the microcavity center illuminated with white light in (b) reflection and (c) transmission on M_1. (d) The local mirror spacing *L(x, y)* is extracted from the measured spectral transmission maximum *λ(x, y)* using equation (1). The value of the full width at half maximum of the local transmission spectrum measured at normal light incidence (perpendicular to the microcavity mirrors) is indicated by arrows and translates into a local cavity-Q of 30. (Adopted from [7])

Fig. 1(a) shows a schematic of the optical microcavity. We prepared the sample from a polymethyl methacrylate (PMMA) / dichloroethane solution containing purified SWNTs with a diameter distribution ranging from 0.8 nm to 1.8 nm (BuckyUSA). A droplet of the solution was enclosed between two silver mirrors. After evaporation of the dichloroethane, the PMMA film fixed the two mirrors and produced immobilized SWNT structures, spatially separated by distances of the order of one micron. Light passing through the microcavity in the λ /2-regime obeys the transmission condition

$$L(x,y) = \left(1 - \frac{\sum_i \Delta\phi_i\left(d_i, \vartheta, \lambda\right)}{2\pi}\right) \frac{\lambda\left(x,y\right)}{2n_{pol}\cos\vartheta}. \qquad (1)$$

Here, $\Delta\phi_i$ denotes the phase change due to reflection at the respective silver mirror i=1, 2 with thickness d_i and $\sum_i \Delta\phi_i$ was calculated to be ~ 1.3 in the present case. The refractive index of the intracavity medium is n_{pol} (= 1.49 for PMMA). The incidence angle of a parallel light beam with respect to the z-axis shown in Fig. 1(a) is given by ϑ. The transmission condition Eq. (1) yields the local mirror spacing *L(x,y)* from the measured intensity maximum λ (*x*, *y*) of the local on-axis transmission spectrum (see Fig. 1(d)). The concentric interference patterns shown in Fig. 1(b) and (c), respectively, indicate that the mirrors are slightly inclined with respect to each other. As a result, we can spatially address SWNTs for different *L(x,y)* and, hence, local photonic mode densities $\rho_{cav}(L)$. The mirror spacing variation $\Delta L(x,y)/\Delta x, y \cong 10^{-3}$ ensures a planar cavity geometry within the focal diameter (< 0.5 μm) of the microscope objective (*NA* = 1.25).

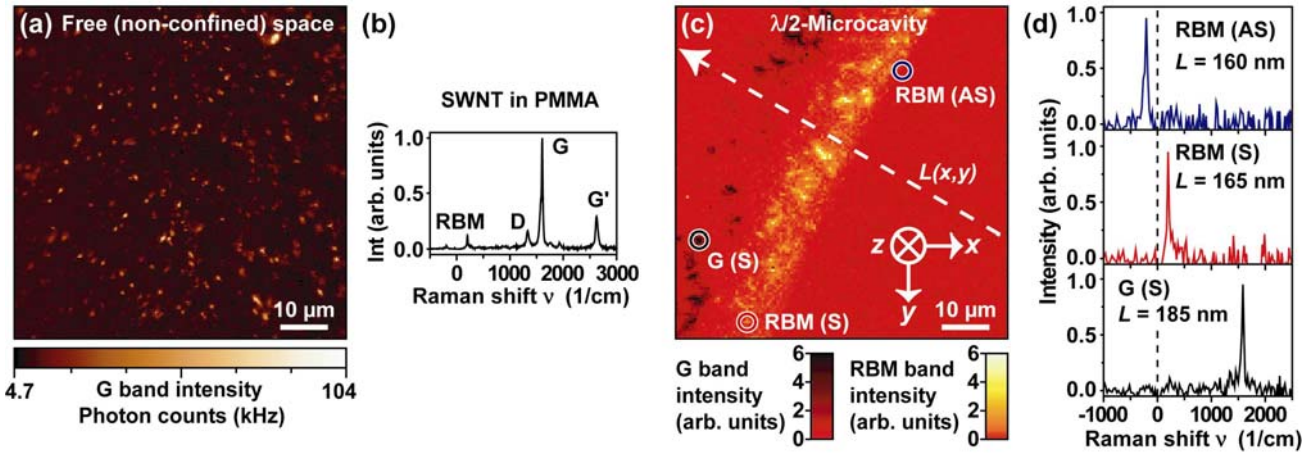

Fig. 2. Raman microscopy and spectroscopy of SWNTs in an optical λ/2-microcavity. (a) Confocal Raman microscopy image of SWNT dispersed in a thin film of PMMA. (b) Raman spectrum of SWNT taken from one of the bright spots in (a). (c) Confocal Raman microscopy image of the same sample as shown in (a), but enclosed between the mirrors of a λ/2-microcavity. Strong scattering intensities of embedded SWNT are obtained where the G band (dark spots) and the RBM band (bright spots) are on resonance with the local photonic mode density $\rho_{cav}(L)$. The direction of increasing mirror spacing *L(x, y)* is indicated by the arrow. (d) Representative microcavity-controlled Raman spectra of SWNT measured at the positions marked in (c) by colored rings {blue: RBM band (anti-Stokes), red: RBM band (Stokes), black: G band (Stokes)}. The laser excitation wavelength is 632.8 nm. (adopted from [7])

As a reference, Fig. 2(a) shows a confocal optical Raman microscopy image of spatially isolated SWNT structures homogeneously distributed in a thin film of PMMA. The Raman spectrum measured on an isolated bright spot is shown in Fig. 2(b) and reveals the vibrational structure of SWNT that is dominated by contributions from the radial breathing vibration (RBM), the disorder-induced vibration (D), its overtone (G') and the C-C stretch vibration (G) [4].

If we use the same PMMA-SWNT solution as the intracavity medium between the mirrors of the λ/2-microresonator, we observe completely different confocal Raman microscopy images. In particular, we find that the scattering intensities for specific vibrational (phonon) modes in SWNT depend on the local mirror spacing *L(x,y)* and, hence, the local photonic mode density $\rho_{cav}(L)$ within the microcavity. To illustrate this spatial dependency, we constructed the Raman image shown in Fig. 2(c) in the following way: For each pixel, a Raman spectrum was acquired and the intensities of the RBM band and the G band were integrated independently and shown in different color scales. We obtain sectors of two spatially separated concentric rings of equal *L*, matching the orientation of the concentric interference pattern as shown in Fig. 1(c): The inner ring is formed by bright spots originating from SWNTs showing strong RBM intensities, the outer ring consists of dark spots that originate from SWNTs showing strong G intensities.

Representative microcavity-controlled Raman spectra taken from the two rings of constant L are shown in Fig. 2(d), together with a spectrum measured for the L corresponding to the RBM anti-Stokes transition. Each spectrum of the SWNT consists of a single Raman band corresponding to the Raman transition that is in resonance with $\rho_{cav}(L)$. The absence of a detectable contribution from the G band in the measured Raman spectra of all SWNTs within the bright inner ring in Fig. 2(c) is the experimental proof for the inhibition of the optical population of the phonon modes associated with the G band by at least one order of magnitude for the broad (n,m)-distribution of the sample material. We calculated the microresonator-controlled Raman scattering cross section for specific Raman transitions of SWNTs [7]. For the microcavity-controlled Raman scattering cross sections for the G-band Anti-Stokes and Stokes transitions, we obtain a maximum ratio of up to 20, depending on the mirror spacing L. This relative change in the Raman scattering cross sections for the G-band transition is a direct consequence of the optical confinement and might be utilized to modify non-equilibrium phonon populations in electrically biased SWNTs.

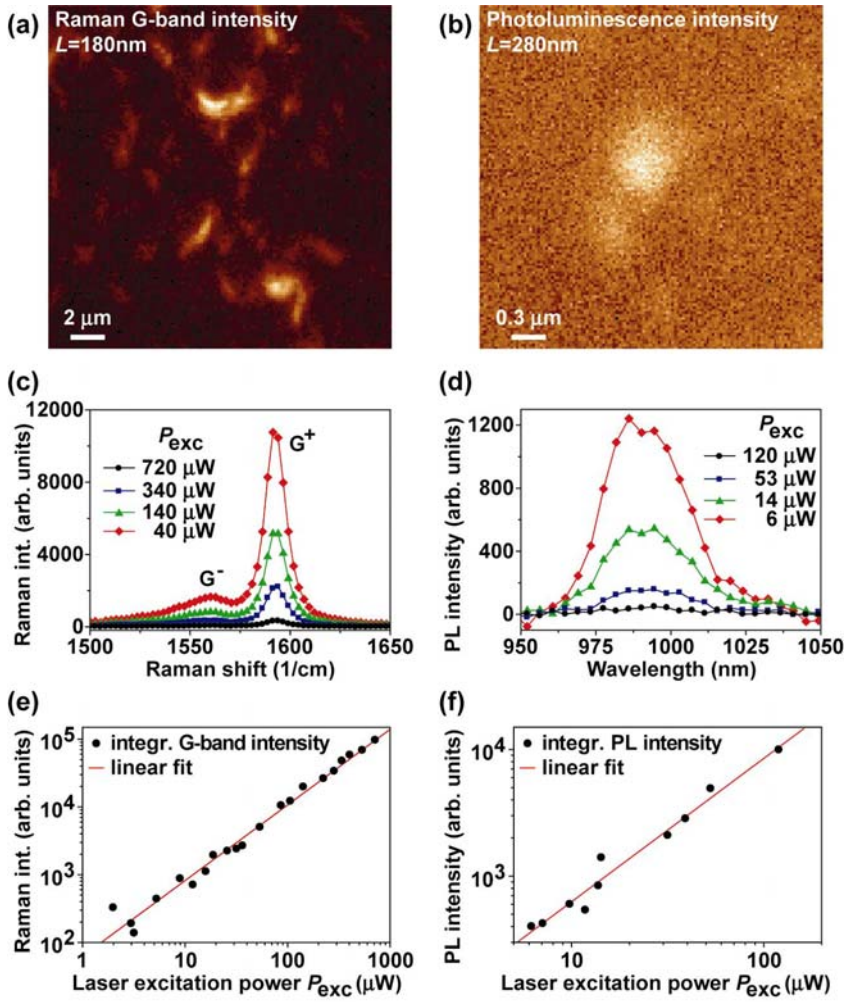

Fig. 3. Microcavity-controlled emission of SWNTs. Confocal optical microscope images show the integrated (a) Raman G-band intensity and (b) photoluminescence (PL) intensity of embedded SWNTs for resonant mirror spacings L. Series of (c) Raman G-band and (d) photoluminescence spectra for different laser excitation powers measured at the position of one of the bright spots in (a) and (b), respectively. To improve the data quality, each Raman and photoluminescence spectrum has been subtracted by a corresponding background spectrum. The integrated intensities derived from the spectra series shown in (c) and (d) are plotted as a function of the laser excitation power in (e) and (f), respectively. The laser excitation wavelength for all measurements is 632.8 nm.

In Fig. 3 (a) and (b), we show Raman scattering (G-band) images as well as photoluminescence (PL) images of SWNTs embedded in the optical microcavity, which have been acquired for SWNT (bundles) located at different microcavity positions, and, hence, different mirror spacings L. For a specific SWNT (bundle), we do not observe Raman scattering and PL simultaneously because of the large spectral separation of the respective emission wavelengths. While the Raman image clearly indicates the extension and in-plane orientation of embedded SWNT (bundles), the PL emission is spatially confined to the extent of the focal spot size of the confocal microscope. As expected, we observe only very few SWNTs with significant PL emission: The efficient transfer of the excited state energy to semiconducting SWNTs having larger diameters or to metallic SWNTs that quench the luminescence emission, makes it very unlikely to observe PL emission in our sample [15, 16]. Figs. 3 (c) and (d) show series of Raman and PL spectra, respectively, acquired from individual bright spots in the scan images Fig. 3 (a) and (b) as a function of the laser excitation power. The measured intensity maximum of the PL spectrum located at about 990 nm indicates emission from a (6,5)-SWNT [17]. In either the Raman G-band or PL spectrum, we do not observe significant line shifts or spectral broadening as we increase the laser excitation power by up to three orders of magnitude. The corresponding integrated intensity curves of the G-band and the PL emission are shown in Fig. 3 (e) and (f) and show linear dependency even for the highest laser powers, indicating that the embedded SWNTs do not heat up significantly. As expected, we do not observe significant microcavity-effects on the spectral line shape of Raman and PL bands, since the corresponding transition linewidths in free (non-confined) space are comparable to or smaller than the spectral widths of available photonic cavity resonances (see figure 1 (d)).

2.2 Electrically excited, microcavity-controlled emission of SWNTs

Even though the major breakthrough of integrating SWNTs into electronic circuits and exciting their luminescence electrically has been achieved already on the single nanotube level [18], the successful application of electrically driven SWNTs in nanophotonics, quantum optics or quantum communications as demonstrated with individual quantum dots [19] is lacking up to now. The control of the radiative properties of current-driven molecular quantum systems like SWNTs by optical confinement remains one of the key challenges in nano-photonics. In the following, we discuss how to integrate a three-terminal field effect transistor field-effect transistor (FET) based on a single, semiconducting SWNT with a planar optical λ/2-microcavity [8].

Fig. 4 (a) shows a three-dimensional schematic of the integrated electronic-photonic nano-device and the corresponding cross-section in Fig. 4 (b) highlights the intensity profile of the longitudinal (forward) cavity mode. The photonic λ/2-microcavity consists of three dielectric layer stacks, i.e. polymethyl methacrylate (PMMA), aluminum oxide (Al_2O_3 deposited by atomic layer deposition) and silicon oxide (SiO_2), placed between a top gold mirror and a parallel bottom silver mirror. The thickness of each optical layer is indicated in Fig. 4 (b). A single SWNT is placed on top of the Al_2O_3 layer close to the microcavity center and is oriented parallel to the silver and the gold mirrors to provide optimum coupling conditions between the SWNT and the longitudinal (forward) mode of the microcavity [14]. The forward mode of the photonic cavity (cavity-Q around 40) is spectrally located at 1.7 microns, designed to overlap with the EL spectrum of the SWNT as measured before deposition of the outcoupling (gold) mirror. The electrical transport characteristics in Fig. 4 (d) shows the drain current versus gate bias for different drain voltages for a representative single CNT-FET. While a conventional silicon-based FET shows unipolar transport characteristics, the SWNT-FET works as a Schottky-barrier-type FET exhibiting ambipolar behavior [20]. For the emission measurements, source and gate electrodes of the SWNT-FET were grounded and the drain electrode was biased at -10 V. The resulting drain current typically ranged between 5 and 10 μA. Under these conditions, electrons are the main type of carrier injected from the drain electrode accumulating kinetic energy in the high-field region near the Schottky-barrier to generate excited states in SWNTs via impact excitation [21], a highly efficient process in one-dimensional structures like SWNTs. The radiative decay of the generated excitons leads to light emission. Before deposition of the top gold mirrors on different SWNT-FETs, we determined the diameter d_t for each individual SWNT from the frequency of the measured Raman transition associated with the RBM [4], delivering d_t-values ranging between 1.2 nm and 2.2 nm. By correlating the measured nanotube diameters with the measured energies of the respective EL intensity maxima ranging between 0.6 eV and 0.8 eV in free (non-confined) space, we find good agreement with the empirical E_{11}-d_t Kataura plot reported in [22].

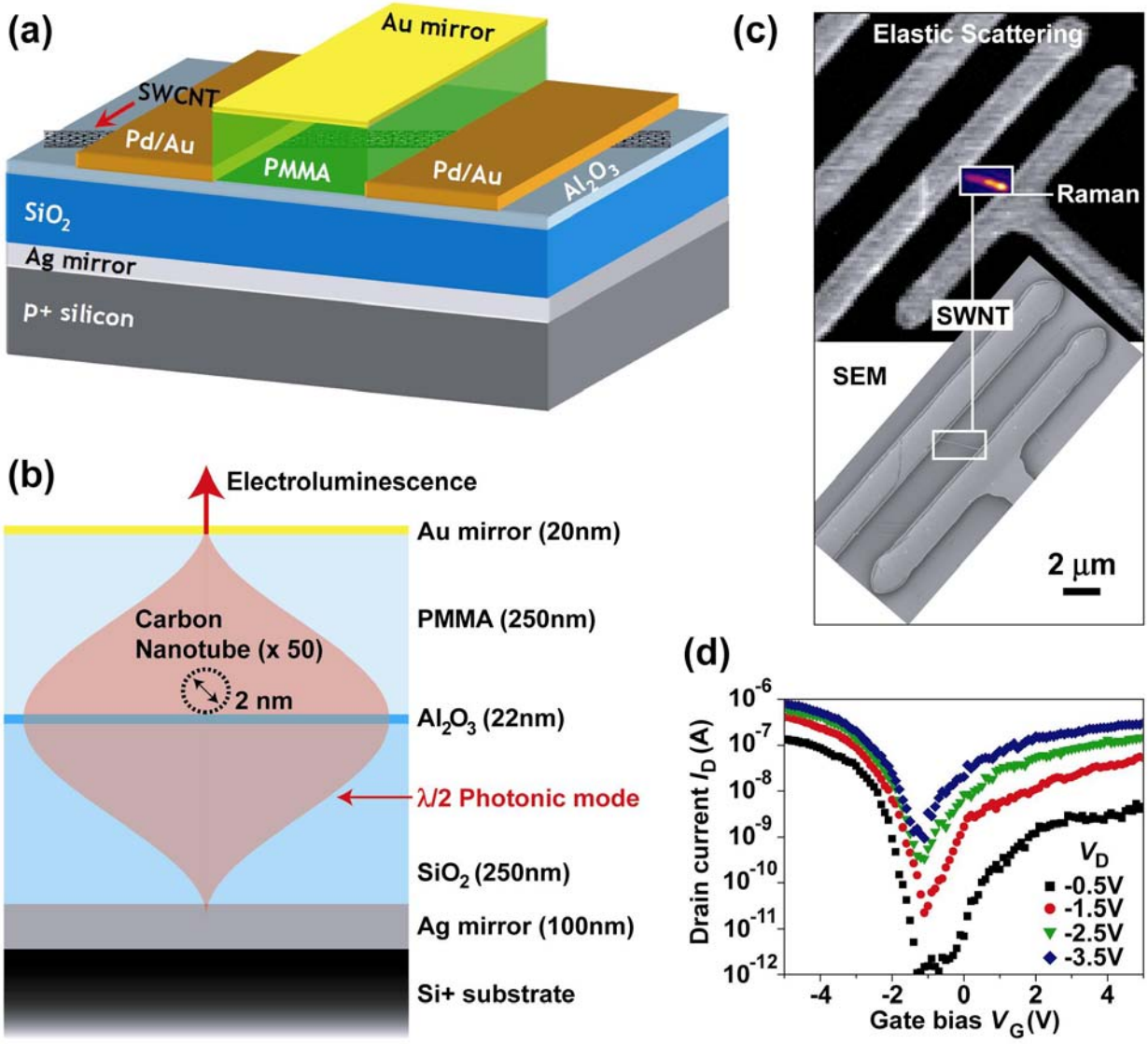

Fig. 4. On-chip integration of a photonic λ/2-microcavity and a field effect transistor (FET) incorporating a single SWNT as an active channel. (a), (b) Device schematics. (c) Elastic and inelastic (Raman) scattering microscopy as well as electron microscopy (SEM) is used for characterizing the SWNT-FET. (c) Electronic device (I-V) characteristics of a SWNT-FET (adopted from [8]).

In Fig. 5 we show the spectral microcavity-effect on the electroluminescence (EL) emission of an individual SWNT-FET. The spectrally broad and spatially undirected EL measured in free space, i.e. before deposition of the top gold mirror (see Fig. 4 (a) and (b)), is transformed into a narrow and nearly symmetric emission band matching the spectral position, line shape and line width of the longitudinal photonic (forward) mode of the photonic cavity. Regardless of the specific structure of individual SWNTs, their free space emissions with a spectral full width at half maximum (FWHM) in the range of 300 nm are spectrally redistributed to produce a narrow and symmetric spectrum with FWHM-values of 40 nm, i.e. in the order of 1/10 of the original value. Moreover, spectral measurements with varying collection apertures (data not shown) demonstrate the increased directionality, or, in other words, the angular narrowing of the microcavity-controlled EL emission. From our model calculations, we estimate a maximum radiative rate (Purcell-) enhancement of four with respect to free (non-confined) space [8].

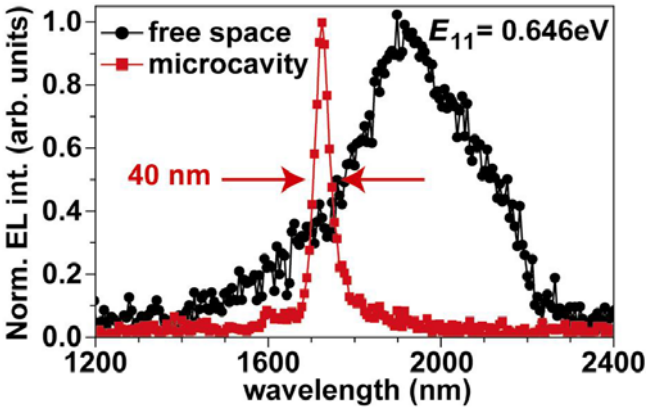

Fig.5. Microcavity-controlled electroluminescence (EL) spectrum of a field-effect transistor (FET) based on a single, semiconducting single-walled carbon nanotube (SWNT). The broad EL spectrum measured from the same SWNT-FET without the optical confinement due to the photonic cavity is shown as a free-space reference. Both spectra are normalized to their respective intensity maximum (adopted from [8]).

3. SUMMARY AND CONCLUSION

We reported emission studies (Raman, photoluminescence, electroluminescence) of individual SWNT (bundles) spatially isolated and immobilized in a planar optical λ/2-microcavity. We demonstrate experimentally that the modified local photonic mode density within the cavity selectively enhances or inhibits different Raman and photoluminescence transitions of embedded SWNTs. For the entire range of laser excitation powers used, we observe a linear power dependence for both resonant (G-band) and PL transitions. Taking into account the recent observation of photon-antibunching in the PL emission of individual SWNT [23], we believe that microcavities can significantly improve the radiative performance of SWNTs for application as single photon sources in quantum optics and quantum communication. The first on-chip integration of an optical λ/2-microcavity and a field-effect transistor based on a semiconducting SWNT, forming a current-driven, highly directed and spectrally narrow infrared nano-light source, constitutes an important step in nanophotonics. SWNT-based light sources may find applications in integrated nanophotonic circuits, quantum optics and on-chip optical interconnects.

4. ACKNOWLEDGMENTS

We thank M. Freitag, Yu. A. Vlasov, S. Assefa, and W. G. Green (all IBM T. J. Watson Research Center), A. Jorio (UFMG, Belo Horizonte, Brazil) and A. K. Swan (BU, Boston, USA) for helpful discussions, J. Tsang, M. Kinoshita and J. Small (all IBM T. J. Watson Research Center) for experimental support, B. Ek (IBM T. J. Watson Research Center) for technical support, D. Schupp (LMU, Munich, Germany) for help with sample preparation and Central Scientific Services (IBM T. J. Watson Research Center) for metal deposition and mask fabrications. Parts of this work were financially supported by the DFG (Me 1600/6-1/2).

REFERENCES

[1] Jorio, A., Dresselhaus, M. S. and Dresselhaus, G. (eds.), [Carbon Nanotubes: Advanced Topics in the Synthesis, Structure, Properties and Applications], Springer Verlag, Berlin (2008).

[2] Avouris, Ph., Chen, Z. and Perebeinos, V., "Carbon-based electronics," Nature Nanotechnology 2, 605-615 (2007).

[3] Avouris, Ph., Freitag, M. and Perebeinos, V., "Carbon-nanotube photonics and optoelectronics," Nature Photonics 2, 341-350 (2008).

[4] Dresselhaus, M.S., Dresselhaus, G., Saito, R. and Jorio, A., "Raman spectroscopy of carbon nanotubes." Phys. Reports 409, 47-99 (2005).

[5] Tsang, J. C., Freitag, M., Perebeinos, V., Liu, J. and Avouris. Ph., "Doping and phonon renormalization in carbon nanotubes," Nature Nano. 2, 725-730 (2007).

[6] Steiner, M., Schleifenbaum, F. Stupperich, C., Failla, A. V., Hartschuh, A. and Meixner, A.J., "Microcavity-controlled single-molecule fluorescence," ChemPhysChem 6, 2190-2196 (2005).

[7] Steiner, M., Qian, H., Hartschuh, A. and Meixner, A. J., "Controlling nonequilibrium phonon populations in single-walled carbon nanotubes," Nano Lett. 7, 2239-2242 (2007).

[8] Xia, F., Steiner, M., Lin, Y.-M. and Avouris, Ph., "A microcavity-controlled, current-driven, on-chip nanotube emitter at infrared wavelengths," Nature Nanotechnology (accepted)

[9] Vahala, K. J., "Optical microcavities," Nature 424, 839-846 (2003).

[10] Purcell, E. M., "Spontaneous emission probabilities at radio frequencies," Phys. Rev. 69, 681 (1946).

[11] Kleppner, D., "Inhibited spontaneous emission," Phys. Rev. Lett. 47, 233-236 (1981).

[12] Cairo, F., De Martini, F. and Murra, D., "QED-vacuum confinement of inelastic quantum scattering at optical frequencies: A new perspective in Raman spectroscopy," Phys. Rev. Lett. 70, 1413-1416 (1993).

[13] Fainstein, A.; Jusserand, B.; Thierry-Mieg, V., "Raman Scattering Enhancement by Optical Confinement in a Semiconductor Planar Microcavity," Phys. Rev. Lett. 75, 3764-3767 (1995).

[14] Yokoyama, H. and Ujihara, K. (eds.), [Spontaneous Emission and Laser Oscillation in Microcavities], CRC Press, Boca Raton, FL, (1995).

[15] Tan, P. H., Rozhin, A. G., Hasan, T., Hu, P., Scardaci, V., Milne, W. I. and Ferrari, A. C., "Photoluminescence Spectroscopy of Carbon Nanotube Bundles: Evidence for Exciton Energy Transfer," Phys. Rev. Lett. 99, 137402 (2007).

[16] Qian, H., Georgi, C., Anderson, N., Green, A. A., Hersam, M. C., Novotny, L. and A. Hartschuh, "Exciton Energy Transfer in Pairs of Single-Walled Carbon Nanotubes," Nano Lett. 8, 1363-1367 (2008).

[17] Leeuw, T. K., Tsyboulski, D. A., Nikolaev, P. N., Bachilo, S. N., Arepalli, S. and Weisman, B., "Strain Measurements on Individual Single-Walled Carbon Nanotubes in a Polymer Host: Structure-Dependent Spectral Shifts and Load Transfer," Nano Lett. 8, 826-831 (2008).

[18] Misewich, J. A., Martel, R., Avouris, Ph., Tsang, J. C., Heinze, S. and Tersoff, J., "Electrically induced optical emission from a carbon nanotube FET," Science 300, 783–786 (2003).

[19] Yuan, Z., Kardynal, B. E., Stevenson, R. M., Shields, A. J., Lobo, C. J., Cooper, K., Beattie, N. S., Ritchie, D. A. and Pepper, M., "Electrically Driven Single-Photon Source," Science 295, 102-105 (2002)

[20] Martel, R., Derycke, V., Lavoie, C., Appenzeller, J., Chan, K. K., Tersoff, J. and Avouris, Ph. "Ambipolar Electrical Transport in Semiconducting Single-Wall Carbon Nanotubes," Phys. Rev. Lett. 87, 256805 (2001)

[21] Chen, J., Perebeinos, V., Freitag, M., Tsang, J., Fu, Q, Liu, J. and Avouris, Ph. ”Bright Infrared Emission from Electrically Induced Excitons in Carbon Nanotubes,” Science 310, 1171–1174 (2005)

[22] Weisman, R. B. and Bachilo, S. M., “Dependence of Optical Transition Energies on Structure for Single-Walled Carbon Nanotubes in Aqueous Suspension: An Empirical Kataura Plot” Nano Lett. 3, 1235-1238 (2003).

[23] Högele, A., Galland, C., Winger, M. and Imamoğlu, A., “Photon Antibunching in the Photoluminescence Spectra of a Single Carbon Nanotube,” Phys. Rev. Lett. **100**, 217401 (2008)